DISSERTATION

EVIDENCE FOR THE ROLE OF DELTA-6-DESATURASE IN THE DEVELOPMENT OF CARDIOMETABOLIC DISEASE.

Submitted by

Christopher Myles Mulligan

Department of Food Science and Human Nutrition

In partial fulfillment of the requirements

For the degree of Doctor of Philosophy

Colorado State University

Fort Collins, Colorado

Summer 2014

Doctoral Committee:

Advisor: Adam J. Chicco

Mary Harris
Melinda Frye
Jairam Vanamala

ABSTRACT

EVIDENCE FOR THE ROLE OF DELTA-6-DESATURASE IN THE DEVELOPMENT OF CARDIOMETABOLIC DISEASE.

The following investigation comprises a series of experiments with the overall aim of elucidating the role of delta-6-desaturase (D6D) in the development of cardiometabolic disease. The experiments tested the general hypothesis that changes in fatty acid membrane composition found to be associated with cardiometabolic disease are attributed to delta-6-desaturase activity and contribute to the development of disease. The specific aims of each experimental series were to: 1) Determine whether inhibition of D6D *in vivo* in established models of heart failure and type 2 diabetes (T2D) reverses changes in fatty acid membrane composition associated with disease pathogenesis and attenuates associated cardiometabolic insults, and 2) Determine whether over-expression of *fads2*, the gene that encodes for D6D, results in altered membrane fatty acid composition and the development of metabolic insults associated with (T2D). Studies in aim 1 demonstrated that the changes in fatty acid membrane composition observed in heart failure and T2D/insulin resistance are a result of increased metabolism of polyunsaturated fatty acids (PUFAs) through D6D, the rate limiting enzyme in the PUFA metabolism pathway. Pharmacological inhibition of D6D with SC-26196 reversed the aberrant fatty acid membrane composition, reduced myocardial hypertrophy and preserved contractile function in the rodent model of heart failure, and improved glucose tolerance in the rodent model of T2D/insulin resistance. Studies in aim 2 demonstrated D6D as not only a contributor to metabolic disease but a key driver of its development. The animal model of genetic *fads2* over-expression, the gene that encodes for D6D, develops significant glucose and insulin intolerance with age and has

significantly elevated blood lipid levels. Collectively, these findings provide substantial evidence for the role of D6D in phospholipid fatty acid membrane composition and the development and progression of cardiometabolic disease.

TABLE OF CONTENTS

CHAPTER 1-INTRODUCTION AND EXPERIMENTAL AIMS

A well-established characteristic of disease states such as cardiovascular disease and type 2 diabetes (T2D) is an alteration in membrane phospholipid fatty acid composition. Interestingly, despite distinct etiologies and possible genetic variation, the pattern of fatty acid remodeling has consistently manifested as a marked decrease in linoleic acid (18:2n6; LA) with often corresponding increases in long-chain highly unsaturated fatty acids such as arachidonic acid (20:4n6; AA) and/or docosahexaenoic acid (22:6n3; DHA). Due to the fact that these fatty acids are substrates and products of long-chain polyunsaturated fatty acid (PUFA) biosynthesis, it is hypothesized that changes in membrane composition associated with various chronic diseases may result from increased activation of this pathway. The rate-limiting enzyme of this pathway (Fig. 1) is Delta-6-Desaturase (D6D) which drives the endogenous production of the highly unsaturated n-6 and n-3 fatty acids, AA and DHA from the dietary essential fatty acids, linoleic acid and alpha linolenic acid (18:3n3; ALA), respectively. An increase in the AA/LA ratio in serum and tissue phospholipids, a common surrogate marker of D6D activity, has been shown to be highly predictive of incidence of cardiovascular and metabolic disease. This notion is further supported in recent epidemiological studies reporting the association of differences in membrane AA/LA ratio with a common single nucleotide polymorphisms (SNPs) in the gene that encodes for D6D (*fads2*). These studies showed that *fads2* SNPs associated with increased serum fatty acid product/ precursor ratios (e.g., AA/LA), indicative of D6D hyperactivity, are predictive of incidence of inflammation, insulin resistance/T2D, and cardiovascular disease. While there is abundant evidence that elevated AA/LA ratios coincides with markers and incidence of disease, correlation does not mean causation. The mechanism by which these

alterations occur and whether they have any pathophysiological significance was a primary focus of the studies comprising this dissertation.

This body of work provides evidence for an important role of D6D activity in the altered fatty acid membrane composition and associated pathophysiology of cardiometabolic disease. Studies conducted as part of this dissertation research addressed the following hypotheses and specific aims.

Overall hypothesis: Delta-6-Desaturase plays a central role in determining tissue phospholipid fatty acid composition, and elevation of its activity plays an important role in the development of cardiometabolic diseases.

Specific Aims

Specific Aim 1: Determine whether inhibition of D6D *in vivo* in established models of heart failure and T2D reverses changes in fatty acid membrane composition associated with disease pathogenesis and attenuates associated cardiometabolic insults.

Specific Aim 2: Determine whether over-expression of *fads2*, the gene that encodes for D6D, results in altered membrane fatty acid composition and the development of metabolic insults associated with T2D.

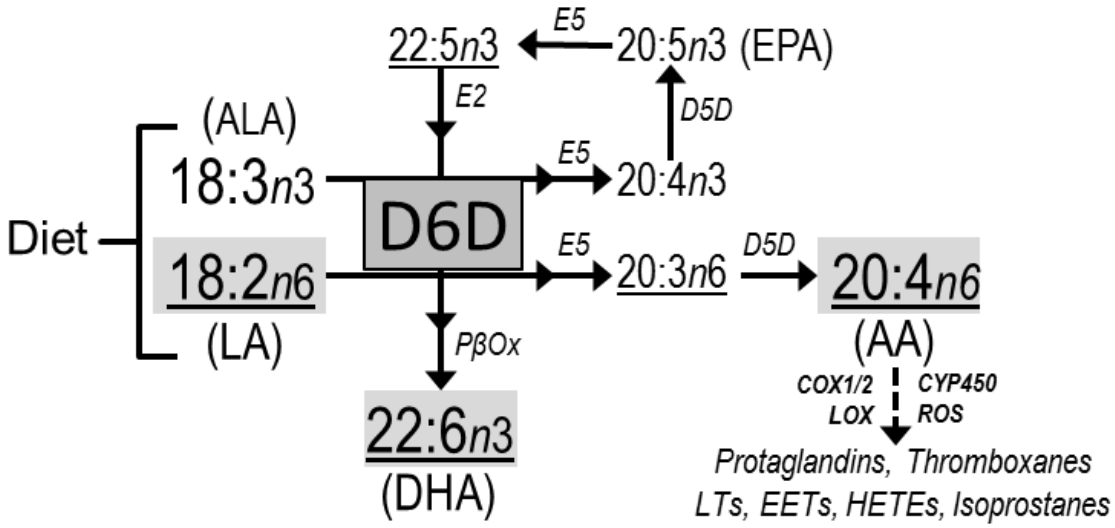

Figure 1. Central role of D6D in PUFA metabolism. Delta-6 desaturase (D6D) catalyzes rate limiting steps in the production of long chain PUFAs from linoleic (18:2*n*6, LA) and linolenic (18:3*n*3) acids obtained in the diet. Double arrows indicate additional reactions catalyzed by elongase enzymes (E), delta-5 desaturase (D5D) and peroxisomal fatty acid β-oxidation (PβOx). LA, AA and DHA (shaded) are the only PUFAs that readily accumulate in cardiac phospholipids to >2% of total fatty acids in humans and rats. Underscored fatty acids are pathway products or precursors routinely used to estimate D6D activity in tissues. AA serves as the substrate for lipoxygenase (LO), cyclooxygenase (COX), and CYP450 epoxygenase enzymes generating an array of bioactive eicosanoid species.

CHAPTER II – THE EFFECT OF DELTA-6-DESATURASE INHIBITION ON MEMBRANE FATTY ACID COMPOSITION AND CARDIOMETABOLIC DISEASE.

Introduction

Alterations in the fatty acid composition of serum and tissue membrane phospholipids have been widely reported in cardiometabolic disorders in human and animal studies. Epidemiological studies have demonstrated strong positive correlations between serum PUFA product/precursor ratios reflective of systemic D6D activity (e.g., AA/LA) with insulin sensitivity (HOMA-IR)(1), body mass index (BMI)(1, 2), childhood obesity(3, 4), impaired fasting glucose(5), incident T2D (6, 7), and the development of metabolic syndrome(8-11). Serum D6D indices also correlate positively with LDL oxidation in type 2 diabetics(12), hyperlipidemia and hyperinsulinemia in fatty liver disease(2) and independently predict CVD incidence and mortality(13-16). Collectively, these studies suggest that D6D activity may represent a novel link between and/or important an prognostic indicator of cardiovascular and/or metabolic disease risk. However, to date, no published experimental studies have directly examined the role of D6D activity in the pathogenesis of cardiac and/or metabolic associated diseases. Studies in this dissertation tested the hypothesis that chronic administration of an orally active D6D inhibitor would attenuate insults associated with T2D, serum pro-inflammatory eicosanoid accumulation, and reduce maladaptive remodeling in hearts in rodent models of obesity/insulin resistance (*ob* mice), and heart failure (SHHF rats), respectively.

Effect of D6D inhibition on SHHF rats with Heart Failure

This study explored the hypothesis that the redistribution of phospholipid PUFAs and maladaptive left ventricular remodeling of the pressure overloaded and failing heart results from increased activity of D6D, the rate-limiting enzyme in the production of long-chain PUFAs such as AA and DHA from LA and α-linolenic acid, respectively (17) (Fig. 1). Herein, we investigated the effects of chronic pharmacological D6D inhibition in rodent models of pressure overload hypertrophy and hypertensive heart disease and present the first comprehensive analysis of phospholipid composition in the failing human heart with and without mechanical unloading support.

Experimental Procedures

Human Heart Tissue

Left ventricular tissue was obtained by an Institutional Review Board-approved protocol maintained by the University of Colorado Denver Cardiac Tissue Bank. Hearts donated for research purposes were obtained under written consent from family members of organ donors or by direct written consent from patients undergoing cardiac transplantation.

Animal Models

Lean male spontaneously hypertensive heart failure (Mcc$^{facp-/-}$; SHHF) rats were obtained from a colony maintained at the University of Colorado. SHHF rats were selected for these studies based on their well-characterized development of progressive hypertensive cardiomyopathy that shares many of the hallmark biochemical and pathophysiological features of dilated cardiomyopathy (DCM) in humans(18). Two cohorts of animals were studied: 1) at

21-22 months of age when rats exhibit pathologic cardiac hypertrophy progressing toward dilated heart failure (HF), and 2) following thoracic aortic banding at 3 months of age to induce hemodynamic stress and pathologic hypertrophy in the absence of age-related pathology (TAC)(19). Cohorts of HF and TAC (2 weeks post-surgery) animals were each divided and matched on echocardiography parameters before being semi-randomly assigned to receive the D6D inhibitor (SC) or no drug for 4 weeks. The effect of the D6D inhibition was also examined in 3 month old SHHF rats exposed to a sham TAC surgery (Sham) that were followed along with TAC groups for 4 weeks as an experimental control. All animals were provided Purina 5001 chow and water ad libitum for the duration of the study. At the conclusion of the study, animals were sacrificed with a lethal dose of sodium pentobarbital (150 mg/kg i.p.) followed by midline thoracotomy and removal of the heart. All procedures were approved by the Animal Care and Use Committee at Colorado State University and/or University of Colorado Boulder in strict compliance with the *Guide for the Care and Use of Laboratory Animals* published by the US National Institutes of Health (NIH Publication No. 85-23, revised 1996).

Inhibition of D6D in vivo

Rats were administered the potent, orally active D6D inhibitor SC-26196 (a gift from Dr. Mark Obukowicz, Pfizer Corporation), at a dose previously reported to selectively inhibit D6D enzyme activity with no effect on other desaturase enzymes in rodents *in vivo* (100 mg/kg/d mixed in chow for 4-weeks), based on daily food consumption records taken over 3-4 weeks prior to treatment (20).

Echocardiography and Blood Pressure

Transthoracic echocardiography was performed under light isoflurane anesthesia prior to and following the 4-week experimental period using a 12 MHz pediatric transducer connected to a Hewlett Packard Sonos 5500 Ultrasound as previously described (21). Tail cuff blood pressure measurements were obtained in the Sham and HF groups using the Kent Coda 6 system (Kent Scientific, Torrinton, CT) in lightly isoflurane-anesthetized rats.

Lipid analyses

See the Appendix I for a detailed description of lipid analyses. Briefly, phospholipids were extracted by thin layer chromatography (total) or liquid chromatography (individual species) for compositional analysis by gas chromatography (fatty acid composition). Myocardial contents of free AA and eicosanoid species were quantified in lipid extracts obtained from 50 mg of LV tissue by LC/MS/MS methods using deuterated standards as previously described in Dr. Robert Murphy's lab at UC Denver (22).

Statistical analyses

All data are presented as group means ± standard error. Human heart data were compared by one-way ANOVA with Tukey tests *post hoc* when appropriate. Rat data were analyzed by 3(condition) X 2(drug) ANOVA to determine main and interaction effects with Tukey tests *post hoc* for determination of significant group differences. Within-group differences in echocardiography data from pre- to post-treatment were compared by paired t-tests. Statistical significance was established at $P < 0.05$ for all analyses.

Results

Phospholipid indices of D6D activity are elevated in the failing human heart and are reversed by mechanical unloading

Compositional analysis of myocardial phospholipids was performed from age-matched individuals with no cardiac pathology (NF; n = 8) and from patients with dilated cardiomyopathy (DCM; n = 8) with or without mechanical unloading with a left ventricular assist device for at least 4 months prior to explantation (LVAD; n = 4) (Fig 1.1). Hearts from patients with dilated cardiomyopathy demonstrated a marked decrease in total phospholipid LA, with corresponding increases in AA, DHA and PUFA product/precursor ratios reflective of D6D hyperactivity compared to donor hearts from NF. LVAD significantly increased phospholipid LA levels while reducing levels of AA, DHA and D6D product/precursor ratios compared to DCM.

D6D inhibition reverses phospholipid PUFA remodeling in TAC and HF

As was seen in the hearts from DCM patients, hearts from TAC and HF rats also demonstrated marked decreases in LA, with parallel increases in AA, DHA, and D6D product/precursor ratio in total myocardial phospholipids compared to Sham controls (Fig 1.2A). Strikingly, chronic administration of the D6D inhibitor ameliorated these effects in both TAC and HF, seen as total myocardial phospholipid LA, AA, and DHA and D6D activity indices returning near to Sham control levels (Fig 1.2B).

Myocardial free arachidonic acid and eicosanoid contents

Once liberated from phospholipids by phospholipase enzymes, AA can serve as a substrate for multiple oxygenase enzymes and non-enzymatic oxidation pathways capable of

generating a host of bioactive eicosanoid species with complex effects on inflammatory, cardiovascular, and transcriptional regulation(23, 24). Both TAC and HF groups elicited significant increases in free AA and several eicosanoid species in the heart, all of which were reduced to near control levels with D6D inhibition (Figure 1.2D). Particularly significant changes were seen in 12- and 15-hydroxyeicosatetraenoic acid, thromboxane A2 (TXA2), and isoprostanes, which are formed via 12-/15-lipoxygenase, cyclooxygenase-2, and the non-enzymatic peroxidation of AA by reactive oxygen species, respectively.

D6D inhibition attenuates maladaptive cardiac remodeling and contractile dysfunction

Echocardiography performed before and after the 4-week experimental period revealed significant progression of left ventricular dilatation and contractile dysfunction in the untreated TAC and HF animals that were significantly attenuated or reversed by D6D inhibition (Fig 1.3A, B). These improvements corresponded to lower final heart and lung weights in the treated compared to untreated animals (Fig 1.3C). Similarly, various measures of cardiac pathology and maladaptive remodeling were shown to be attenuated by D6D inhibition in studies conducted by members of the Chicco lab and collaborators (data not shown; published in (25)). These include reductions in myocardial fibrosis, assessed by tissue hydroxyproline content, histological evidence of reduced interstitial and perivascular collagen deposition, attenuated mRNA expression of atrial natriuretic peptide (ANP) and myocardial extracellular-regulated activated kinase 1/2 (ERK1/2) phosphorylation compared to untreated TAC and HF, and model specific effects on myocardial activation of nuclear factor kappa B (NFκB).

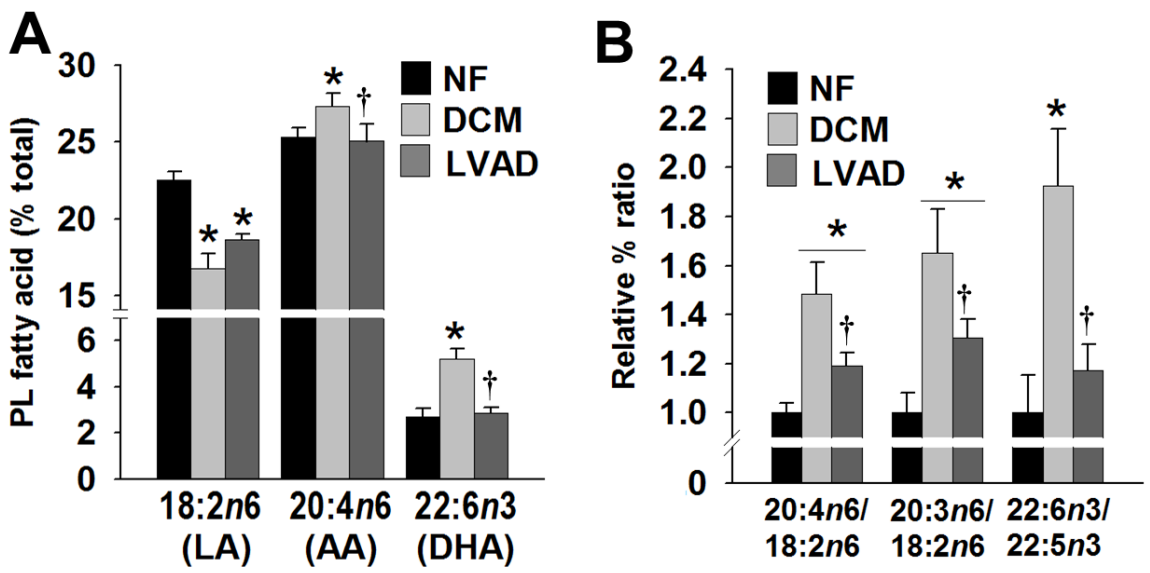

Figure 1.1. Phospholipid PUFA desaturation in human heart failure. Gas chromatographic analysis of total phospholipid fatty acids extracted from human left ventricular tissue revealed a loss of phospholipid LA paralleled by elevations in AA, DHA and PUFA product/precursor ratios in hearts explanted from patients with dilated cardiomyopathy (DCM; n = 8) compared to non-failing donor hearts (NF; n = 8), which was partially reversed in patients implanted with a left ventricular assist device for 4-10 months (LVAD; n = 4). * $P < 0.05$ vs. NF. † $P < 0.05$ vs. DCM.

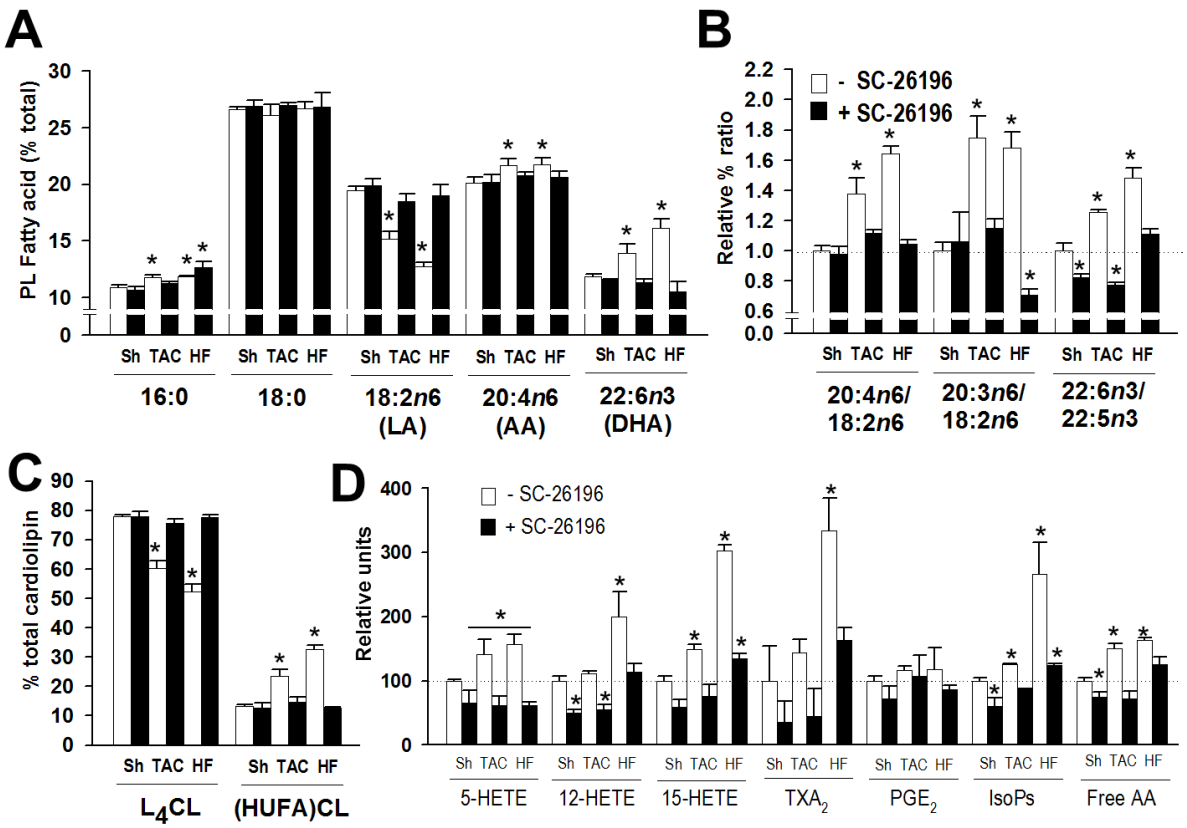

Figure 1.2. Myocardial phospholipid composition and eicosanoids. Treatment of TAC and HF animals with the selective D6D inhibitor SC-26196 for 4 weeks (black bars) normalized relative proportions of LA, AA and DHA (A), and reversed D6D product/precursor indices (B) in the global myocardial phospholipid pool (n= 8-10/group). C) Mass spectrometry of cardiolipin molecular species revealed a restoration of L_4CL and CL species containing highly unsaturated fatty acids (HUFAs) to control levels in cardiac mitochondria with D6D inhibition (n = 4-6/group). D) SC-26196 treatment significantly attenuated elevations in myocardial unesterifed ("free") AA and several of its pathogenic eicosanoid derivatives (n = 4-6/group). A significant group X drug interaction effect was seen for all analyses except 16:0, 18:0, and PGE_2, therefore only significant group differences vs. Sham control at $P < 0.05$ (*) are indicated for clarity. See text for abbreviations.

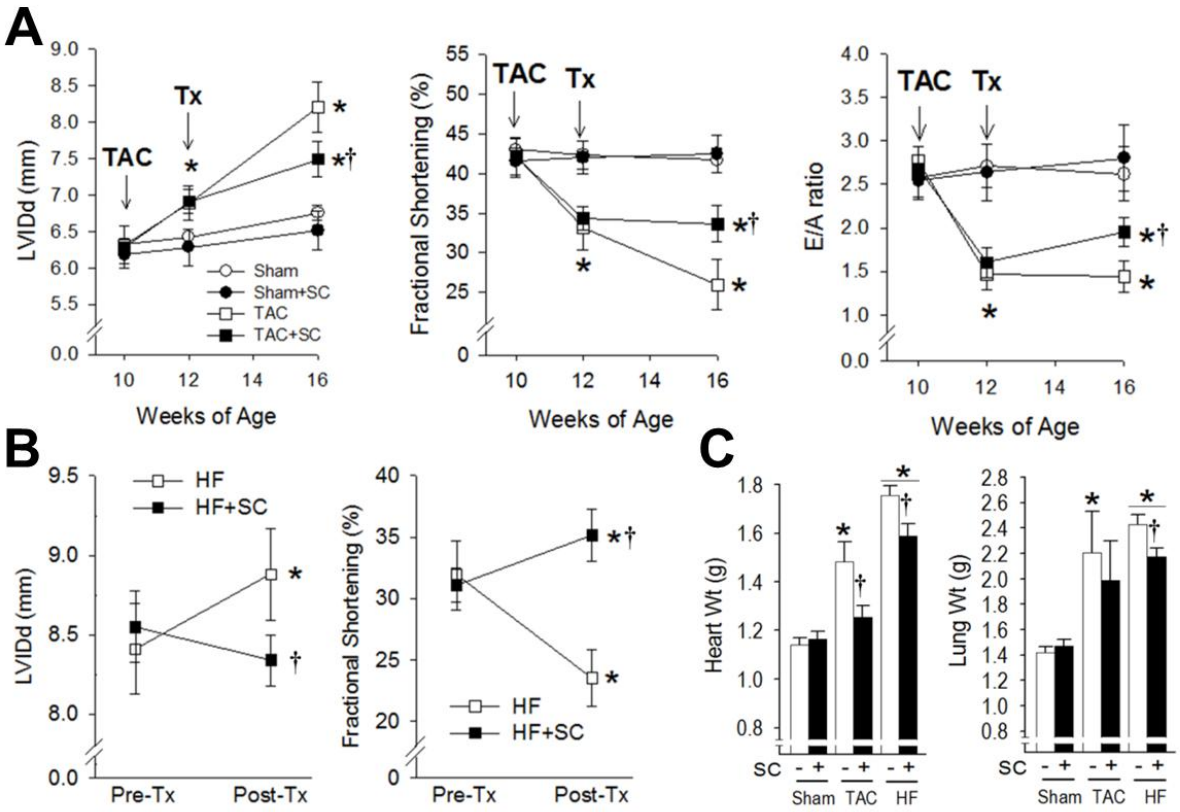

Figure 1.3. D6D inhibition attenuates contractile dysfunction and pathologic hypertrophy in TAC and HF. Serial echocardiography revealed marked left ventricular dilatation (LV internal diameter in diastole, LVIDd), systolic dysfunction (decreased fractional shortening) and diastolic dysfunction (decreased E/A ratio) in TAC animals (n = 8), which was significantly attenuated by D6D inhibition (SC; n=8) beginning 2 weeks following surgery (Tx) (A). LV dilatation and systolic dysfunction in aged SHHF rats (n = 12) during the 4 week experimental period was attenuated or reversed by D6D inhibition (n = 10) (B). SC treatment resulted in significantly lower heart weights in TAC and HF animals, and decreased pulmonary congestion in HF rats (C). * $P < 0.05$ vs. Sham or Pre-Tx HF. † $P < 0.05$ vs. untreated.

Effect of D6D inhibition on murine models of Type 2 Diabetes

This study tested the hypothesis that the redistribution of serum and tissue phospholipid PUFAs and glucose intolerance associated with insulin resistance/T2D results from increased activity of D6D(17). Similar to the experimental design above, the effects of chronic pharmacological D6D inhibition in vivo were examined in the ob/ob mouse model of hyperphagic obesity/T2D.

Experimental Procedures

Animal Model

Eight week old C57Bl/6 and ob/ob mice were obtained from the Jackson Laboratory (JAX) and housed in the Laboratory Animal Resource Facility at Colorado State University (CSU, Fort Collins, Colorado, USA). The mice were fed a standard chow diet for 8 weeks. At 16 weeks of age, the mice were weighed and monitored, and a glucose tolerance test (GTT) was performed. The C57Bl/6 mice were separated into two groups: control (con; n = 6), and control + sc-26196 (consc; n = 6). The ob/ob mice were separated into two groups: obese (ob; n = 6) and obese + sc-26196 (obsc; n = 6). In the con and ob groups, the mice were fed ad libitum a standard chow diet, while those in the consc and obsc groups were fed ad libitum powdered chow containing 100mg/kg sc-26196 for the next 4 weeks of the study. During the 4-week duration of the study, the food intake and body weights were monitored and recorded on a daily basis. Following week 4 of the study, a post-treatment GTT was performed on all groups, after which the mice were sacrificed.

Inhibition of D6D in vivo

Mice were administered the potent, orally active D6D inhibitor SC-26196 (a gift from Dr. Mark Obukowicz, Pfizer Corporation), at a dose previously reported to selectively inhibit D6D enzyme activity with no effect on other desaturase enzymes in rodents *in vivo* (100 mg/kg/d mixed in chow for 4-weeks), based on daily food consumption records taken over 3-4 weeks prior to treatment (20).

Glucose Tolerance Tests

To assess glucose tolerance by GTT, mice were fasted for 6 hours prior to testing and weighed immediately prior to glucose administration (1g/kg body weight i.p.). Mouse tails were gently cleansed and swabbed and a small venous incision was made approximately 2 cm distal to the base of the tail for the collection of blood (1-3 ul). A baseline blood glucose level reading was taken prior to injection at time zero using the Alphatrak glucometer and strips specially designed for use in mice (Abbott Animal Health). Subsequently, glucose was measured every 30 minutes post-injection for 2 hours for a total of five blood glucose readings.

Tissue phospholipid fatty acid composition

See the Appendix I for a detailed description of lipid analyses. Briefly, lipids from heart, muscle, liver and serum (n=4-6/group) were extracted in methanol on ice in the presence of butylated hydroxytoluene (BHT). Methyl esters were obtained by adding sodium methoxide to each sample for gas chromatography (GC) analysis. GC analysis was performed using an Agilent Technologies DB-225 30m x 0.250mm x 0.25μm column (model 122-2232, J&W Scientific) on an Agilent 6890 Series Gas Chromatographer.

Eicosanoid profile

Serum and hepatic contents of free AA, and 36 eicosanoid species derived from AA were quantified in lipid extracts obtained from 200 μL of serum or liver homogenates with the assistance of Dr. Robert Murphy's laboratory at the University of Colorado Denver using LC/MS/MS as previously described in detail (19, 26) Mass transitions for 36 eicosanoid species have been established using this method, including all of the major COX and LOX pathway products (PGs, HETEs, LTs, TXs, EETs), using a deuterated standards (Cayman) on a normal-phase HPLC column (Prodigy 5 μm silica 100 Å, 1.0 × 150 mm column; Phenomenex) coupled to a API 2000 mass spectrometer (MS) at the University of Colorado using MultiQuant software (AbSciex) for analyses of MS data.

Immunoblotting

See the Appendix I for a detailed description of immunoblotting methods. Briefly, liver tissue was probed for IRS-1, ^{ser307}pIRS-1, c-Jun N-terminal kinases (JNK) and pJNK using commercially available antibodies (Cell signaling or Santa Cruz) using standard immunoblotting methods routinely performed in the Chicco lab.

Serum analyses

Serum insulin levels were quantified using commercially available colorimetric/ELISA kits (BioVision, Crystal Chem) according to the manufacturer's instructions. Mice were fasted 6 hrs prior to serum collection at the time of animal sacrifice, aliquoted, and stored at -80C for future analyses.

Results

D6D inhibition reverses phospholipid PUFA remodeling in Obesity/Insulin Resistance

Heart, muscle, liver, and serum from ob/ob (n = 4-6/group) mice demonstrated marked decreases in LA, with parallel increases in AA, DHA, and D6D product/precursor ratio in total phospholipids compared to controls. As hypothesized, chronic administration of the D6D inhibitor ameliorated these effects in the ob/ob mouse, seen as phospholipid AA/LA ratio, indicative of D6D activity returning near to control levels (Fig 2.1A). SC-26196 treatment significantly attenuated elevations in several pro-inflammatory eicosanoid derivatives in ob mice to near control levels (Fig. 2.1B).

D6D inhibition improves markers of Type 2 Diabetes

An animal is considered glucose tolerant when its ability to adequately dispose of a given glucose load after 2 hours is not statistically different than that of a control animal. Glucose tolerance prior to D6D inhibition was significantly impaired in the ob/ob mice compared to controls. Following 4 weeks of supplementation with the D6D inhibitor glucose tolerance was improved in the ob/ob mouse to near control levels (Fig. 2.2A). The improvement in glucose tolerance corresponded with a lower fasting insulin in the obsc group compared to the ob group (Fig. 2.2B).

D6D inhibition and hepatic insulin signaling

Liver tissue was probed for proteins previously shown to affect insulin signaling using standard western blotting methods. IRS-1 is an important modulator of insulin signaling, but phosphorylation of IRS-1 at serine 307 inhibits insulin signaling to downstream effectors that

mediated GLUT-4 translocation and glucose uptake. Activation of the c-jun N-terminal kinase (JNK) signaling cascade leads to serine phosphorylation of IRS-1 through pJNK. Therefore, an increase in the ratios of ^{Ser307}pIRS-1/IRS-1 and pJNK/JNK are markers of impaired insulin signaling. Hepatic immunoblotting results demonstrated a significant increase in pJNK protein levels were significantly increased in ob mice vs. controls, $p < 0.05$. There was no significant difference in JNK protein among groups. This resulted in a significant increase in the pJNK/JNK ratio in the ob vs. the con, which was returned to control levels following D6D inhibition (Fig. 2.3A). ^{Ser307}pIRS-1 protein levels in ob mice was reversed by SC-26196 treatment, ($p < 0.05$). There were no differences in IRS-1 protein levels among treatment groups. This resulted in a significant increase in the ^{S307}pIRS-1/IRS-1 ratio in the ob vs. the con, which was returned to control levels following D6D inhibition. (Fig. 2.3B)

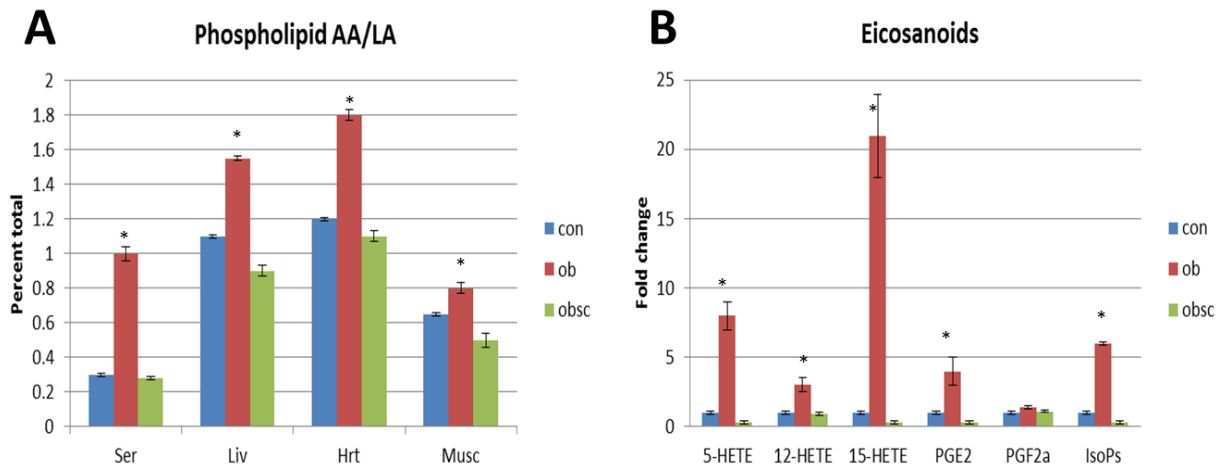

Figure 2.1 D6D inhibition reverses phospholipid AA/LA ratio and eicosanoid profile.

Treatment of ob/ob mice with the selective D6D inhibitor SC-26196 for 4 weeks reverses the elevated AA/LA ratio in serum, heart, liver, and muscle phospholipids (A). SC-26196 treatment significantly attenuated elevations in AA eicosanoid derivatives (B). Significant group differences vs. control at $p < 0.05$ (*) are indicated for clarity.

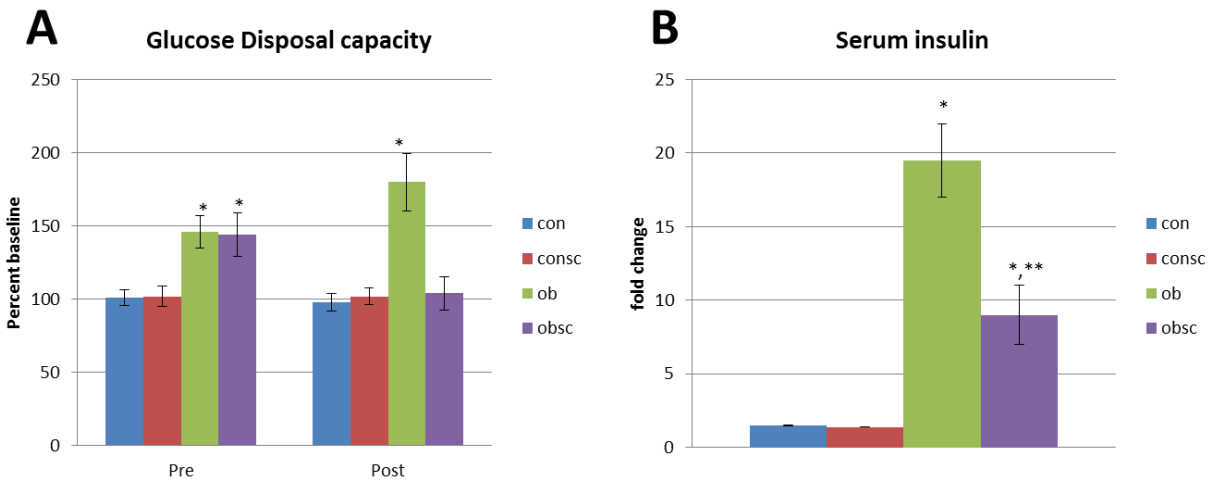

Figure 2.2 D6D inhibition with SC-26196 attenuates glucose disposal capacity and reduces fasting insulin in OB mice. Treatment of ob/ob mice with the selective D6D inhibitor SC-26196 for 4 weeks improved glucose tolerance (A) and reduced fasting insulin levels (B). Significance group differences from control $p < 0.05$ (*) are indicated for clarity. (**) $p < 0.05$ for difference from ob.

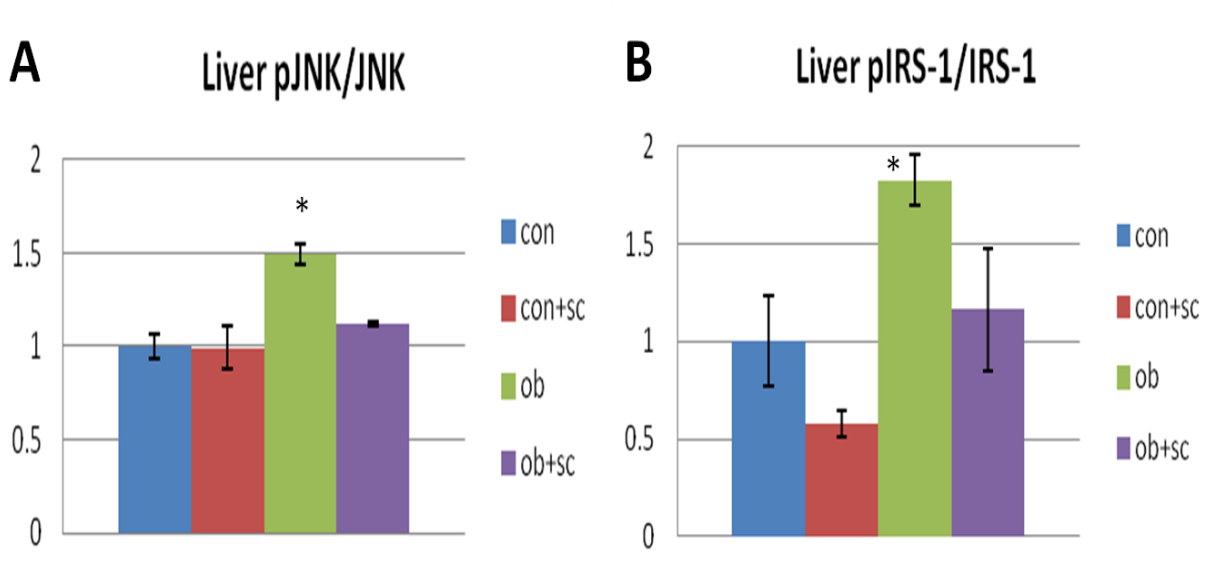

Figure 2.3 D6D inhibition with SC-26196 attenuates reverses impaired insulin signaling in OB mice. pJNK (A) and pIRS-1 (B) protein content in liver of ob/ob mice was significantly elevated compared to wt control mice, and was decreased to control levels following SC-26196 supplementation. Significance group differences from control $p < 0.05$ (*) are indicated for clarity.

Discussion

These studies demonstrate a pivotal role for D6D in generating the signature pattern of phospholipid PUFA redistribution associated with cardiometabolic pathology in experimental models of hypertensive heart disease and obesity/insulin resistance. The remarkable phenotypic effects of D6D inhibition in TAC, HF, and ob/ob animals highlight the pathophysiological importance of this process, and provide novel insight into the mechanisms responsible for maladaptive remodeling and contractile dysfunction in the pressure overloaded myocardium and glucose intolerance in an established model of T2D/insulin resistance. Although previous studies have associated serum markers of D6D activity with coronary artery disease risk(14), inflammation(13), and T2D(1, 27), these studies provide the first experimental evidence for the role of this enzyme in regulating myocardial membrane composition and maladaptive adaptation in models of heart disease, global tissue membrane composition and glucose homeostasis in obesity/insulin resistance.

The proportional loss of phospholipid LA is the most marked and consistent manifestation of membrane remodeling associated with cardiac overload and Type 2 Diabetes/insulin resistance across species, tissues, and phospholipid classes observed herein and in previous studies. The reversibility of this effect by D6D inhibition implicates the conversion of LA into downstream PUFA desaturation/elongation products, the most prominent being AA. However, reciprocal increases in phospholipid AA were not always seen to the same magnitude as LA losses in the aforementioned studies. Importantly, PUFAs must be hydrolyzed from phospholipids by phospholipase A2 enzymes to react with desaturation/elongation enzymes, and are subsequently re-esterified into phospholipids by acyltransferase enzymes with varying substrate specificities(28). Similarly, AA is cleaved from myocardial phospholipids by

phospholipase A2 enzymes for subsequent metabolism as free AA by cyclooxygenase, lipoxygenase, or cytochrome P450 monooxygenase enzymes(23), generating a host of eicosanoid species with diverse biological effects(24).

Arachidonic acid derived eicosanoids have been implicated in the pathogenesis of heart failure. Most notably TXA_2, 12- and 15- hydroxyeicosatetraenoic acid have been well established to be involved in the development of cardiac hypertrophy and contractile dysfunction. These eicosanoids have also been shown to serve as potent initiators and propagators of inflammatory signaling leading to cardiac hypertrophy and heart failure(29, 30).

Eicosanoids are also believed to play a role in the development of insulin resistance/Type 2 Diabetes by initiating an inflammatory response. Eicosanoids initiate a pro-inflammatory response by releasing cytokines into circulation. These cytokines bind to receptors which initiate signaling cascades. A prominent signaling cascade shown to play a role in the development of insulin resistance is JNK. JNK activation is mediated by various inflammatory cytokines and free fatty acids, like AA. Once activated, JNK can phosphorylate IRS-1, an important protein in the insulin signaling cascade, at ser^{307} blocking its activation site and inhibiting insulin signaling(31).

Therefore, D6D inhibition may have attenuated maladaptive remodeling and improved contractile function in models of heart failure and improved glucose tolerance in the model of insulin resistance/T2D by reducing AA production and thereby minimizing the production of pro-inflammatory eicosanoids. Other mechanisms, such as altered mitochondrial function, membrane lipid signaling or protein function, and lipo-oxidative stress, were also examined by other members of the Chicco lab as potential contributors to the phenotypic changes associated

with D6D inhibition in these models. However, these studies are beyond the scope of the dissertation.

CHAPTER III – THE ROLE OF *fads2* OVER-EXPRESSION ON MEMBRANE FATTY ACID COMPOSITION AND CARDIOMETABOLIC DISEASE.

Introduction

The results of the previous studies using a pharmacological delta-6-desaturase (D6D) inhibitor provide abundant evidence for D6D involvement in the progression of cardiometabolic disease. The activity of this enzyme has been shown to be stimulated by a number of different components and consequences associated with metabolic disease including sucrose (32, 33) cholesterol (34) or hydrogenated fat (35) and hyperinsulinemia (36-38) suggesting an increase in D6D activity as part of a broader pathology leading to the development of cardiometabolic disease. Independent of pathologic augmentation of D6D, recent epidemiological studies have reported common single nucleotide polymorphisms (SNPs) in the gene that encodes for D6D (*fads2*) that are associated with differences in membrane AA/LA ratio, suggesting genetic variation of the activity of D6D. These studies found that fads2 SNPs associated with increased serum fatty acid product/precursor ratios (e.g., AA/LA), indicative of D6D hyperactivity, are predictive of incidence of inflammation, insulin resistance/T2D, and cardiovascular disease. It was attempted to determine whether D6D activity is the primary driver of metabolic derangement as it pertains to the development of insulin resistance/glucose intolerance. In an effort to achieve this goal a transgenic mouse model was developed that over-expresses *fads2*, the gene that encodes for D6D. It was hypothesized that *fads2* over-expression will lead to elevations in AA/LA ratios, increased eicosanoid production, and the development of metabolic insults associated with T2D.

Experimental Procedures

Animal model

A line of mice with global transgenic overexpression of the D6D gene, *fads2* was developed in the Chicco lab by Dr. Catherine Le (previous PhD student in the Cell and Molecular Biology Program). Mice were generated using the cytomegalovirus (CMV) promoter to direct overexpression of the transgene globally. Once the *fads2* plasmid DNA was transformed into *E.coli*, isolated plasmid was cut with MfeI and BstBI to excise the 4.3kb transgene fragment that was then purified for pronuclear injection to generate the *fads2OVR* transgenic mouse.

Glucose and Insulin Tolerance Tests

To assess glucose tolerance by GTT, mice were fasted for 6 hours prior to testing and weighed immediately prior to glucose administration (2g/kg body weight i.p.). Mouse tails were gently cleansed and swabbed and a small venous incision was made approximately 2 cm distal to the base of the tail for the collection of blood (1-3 ul). A baseline blood glucose level reading was taken prior to injection at time zero using the Alphatrak glucometer and strip specially designed for use in mice (Abbott Animal Health) followed by subsequent measurements every 30 minutes post-injection for 2 hours for a total of five blood glucose readings. Insulin tolerance tests (ITT) were performed following a 6 hour fast starting at 8 am. Mice were weighed immediately prior to insulin administration (0.5U/kg body weight i.p). Blood glucose measurements were taken as stated above. A baseline blood glucose level reading was taken prior to injection at time zero and again at 15, 30, 60, and 120 minutes post injection.

Fatty acid membrane composition

See the Appendix I for a detailed description of lipid analyses. Briefly, lipids from heart, muscle, liver and serum (n=4-6/group) were extracted in methanol on ice in the presence of BHT. Methyl esters were obtained by adding sodium methoxide to each sample for GC analysis. GC analysis was performed using an Agilent Technologies DB-225 30m x 0.250mm x 0.25μm column (model 122-2232, J&W Scientific) on an Agilent 6890 Series Gas Chromatographer.

Eicosanoid profile

Serum and hepatic contents of free AA, and 36 eicosanoid species derived from AA were quantified in lipid extracts obtained from 200 μL of serum or liver homogenates with the assistance of Dr. Robert Murphy's laboratory at the University of Colorado Denver using LC/MS/MS as previously described in detail (19, 26) Mass transitions for 36 eicosanoid species have been established using this method, including all of the major COX and LOX pathway products (PGs, HETEs, LTs, TXs, EETs), using a deuterated standards (Cayman) on a normal-phase HPLC column (Prodigy 5 μm silica 100 Å, 1.0 × 150 mm column; Phenomenex) coupled to a API 2000 mass spectrometer (MS) at the University of Colorado using MultiQuant software (AbSciex) for analyses of MS data.

Immunoblotting

See the Appendix I for a detailed description of immunoblotting methods. Briefly, muscle and liver tissue was probed for IRS-1, ^{ser307}pIRS-1, JNK and pJNK using commercially available antibodies (Cell signaling or Santa Cruz) using standard immunoblotting methods routinely performed in the Chicco lab.

Serum analyses

Serum samples were analyzed for LDL+VLDL, HDL, total cholesterol, and triglyceride content and were quantified using commercially available colorimetric/ELISA kits (BioVision, Crystal Chem). Mice were fasted 6 hrs prior to serum collection at the time of animal sacrifice, aliquoted, and stored at -80C for future analyses.

Results

Over-expression of fads2 results in phospholipid PUFA remodeling, increased serum lipid concentrations, and elevations in AA derived eicosanoids.

Over-expression of *fads2* lead to a significant increase in the AA/LA ratio in serum, muscle, liver, and heart compared to wt controls (Fig. 3.1A). This was achieved through significant decreases in linoleic acid and trending increases in arachidonic acid in serum and tissue phospholipids (see Table 1 in Appendix I). Furthermore, *fads2* over-expression resulted in significant elevations in several pro-inflammatory eicosanoid derivatives (Fig. 3.1B). This suggests that increased biosynthesis of AA from LA by the D6D pathway is sufficient to increase pro-inflammatory eicosanoid production independent of coexistenting pathology or dietary manipulation. Mice over-expressing *fads2* also had significantly elevated serum triglyceride, HDL, LDL+VLDL, and total cholesterol concentrations (Fig. 3.1C,D).

Over-expression of fads2 leads to impaired glucose and insulin tolerance

Glucose tolerance was significantly impaired in *fads2OVR* mice compared to wild type (wt) controls. Glucose tolerance also significantly declined with age in *fads2OVR*, but not in the wt controls (Fig 3.2A,B,C). Furthermore, there was a trend for insulin intolerance at 2 months

($p<0.07$) in *fads2OVR* mice. By 6 months of age *fads2OVR* mice had a significantly depressed response to an insulin challenge compared to wt controls, which did not differ from 2 months of age (Fig. 3.2D,E,F).

Over-expression of fads2 leads to impaired insulin signaling in muscle and liver

Liver and muscle tissue were probed for proteins previously shown to affect insulin signaling using standard western blotting methods. IRS-1 is an important modulator of insulin signaling, but phosphorylation of IRS-1 at serine 307 leads to impaired insulin signaling. Activation of the JNK signaling cascade leads to serine phosphorylation of IRS-1 through pJNK. An increase in the ratios of ^{Ser307}pIRS-1/IRS-1 and pJNK/JNK are considered markers of impaired insulin signaling. Western blot analysis of liver and muscle tissue demonstrated a significant increase in ^{Ser307}pIRS-1 protein levels in *fads2OVR* mice compared to that of controls ($p < 0.05$). There were no differences in IRS-1 protein levels between groups. This resulted in a significant increase in the ^{Ser307}pIRS-1/IRS-1 ratio in *fad2OVR* vs. wt. (Figure 3.3A and B). pJNK protein levels were also significantly increased in both liver and muscle in *fads2OVR* mice vs. wt ($p < 0.05$). There was no significant difference in JNK protein between groups. This resulted in a significant increase in the pJNK/JNK ratio in *fad2OVR* vs. wt. (Figure 3.3C and D).

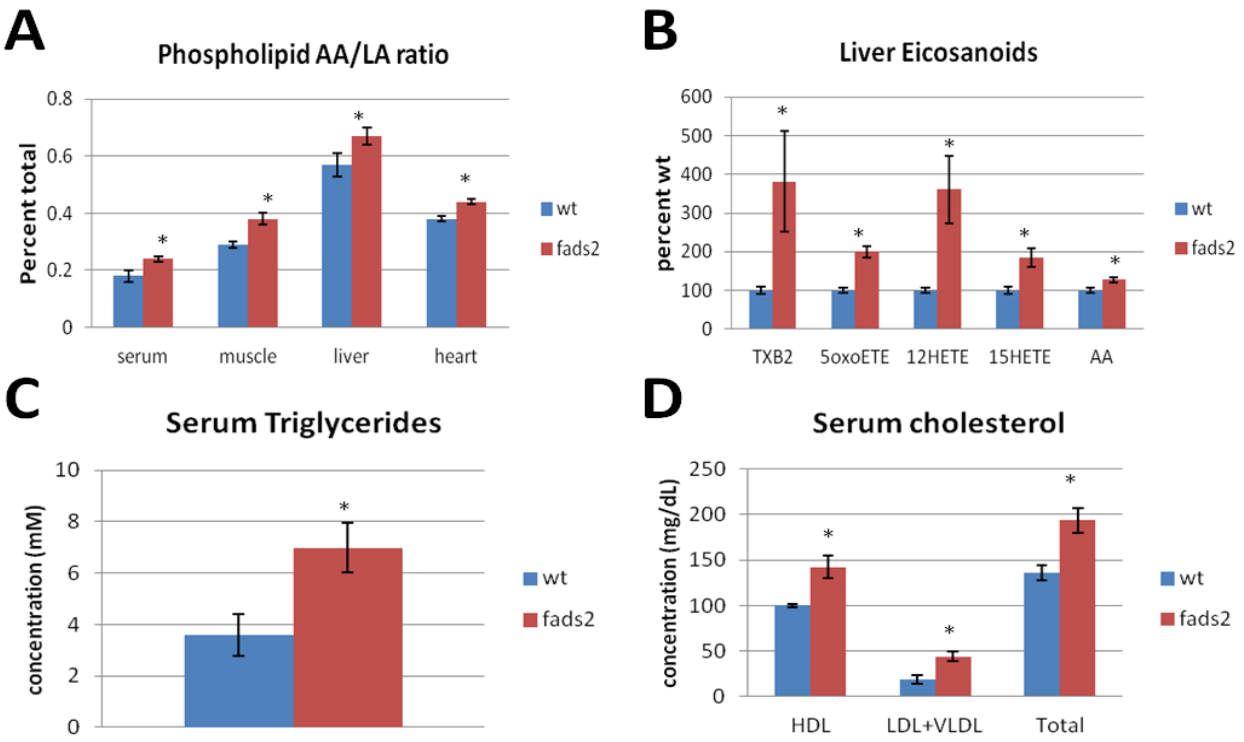

Figure 3.1 Phospholipid AA/LA ratio, eicosanoid profile, and serum lipids following *fads2* over-expression. Genetic over-expression of *fads*2, the gene that encodes for D6D, significantly increases the (A) AA/LA ratio in heart, muscle, liver, and serum (B) AA derived eicosanoids, (C) triglycerides, and (D) serum cholesterol levels compared to wt controls. Significant differences vs. control at $p < 0.05$ (*) are indicated for clarity.

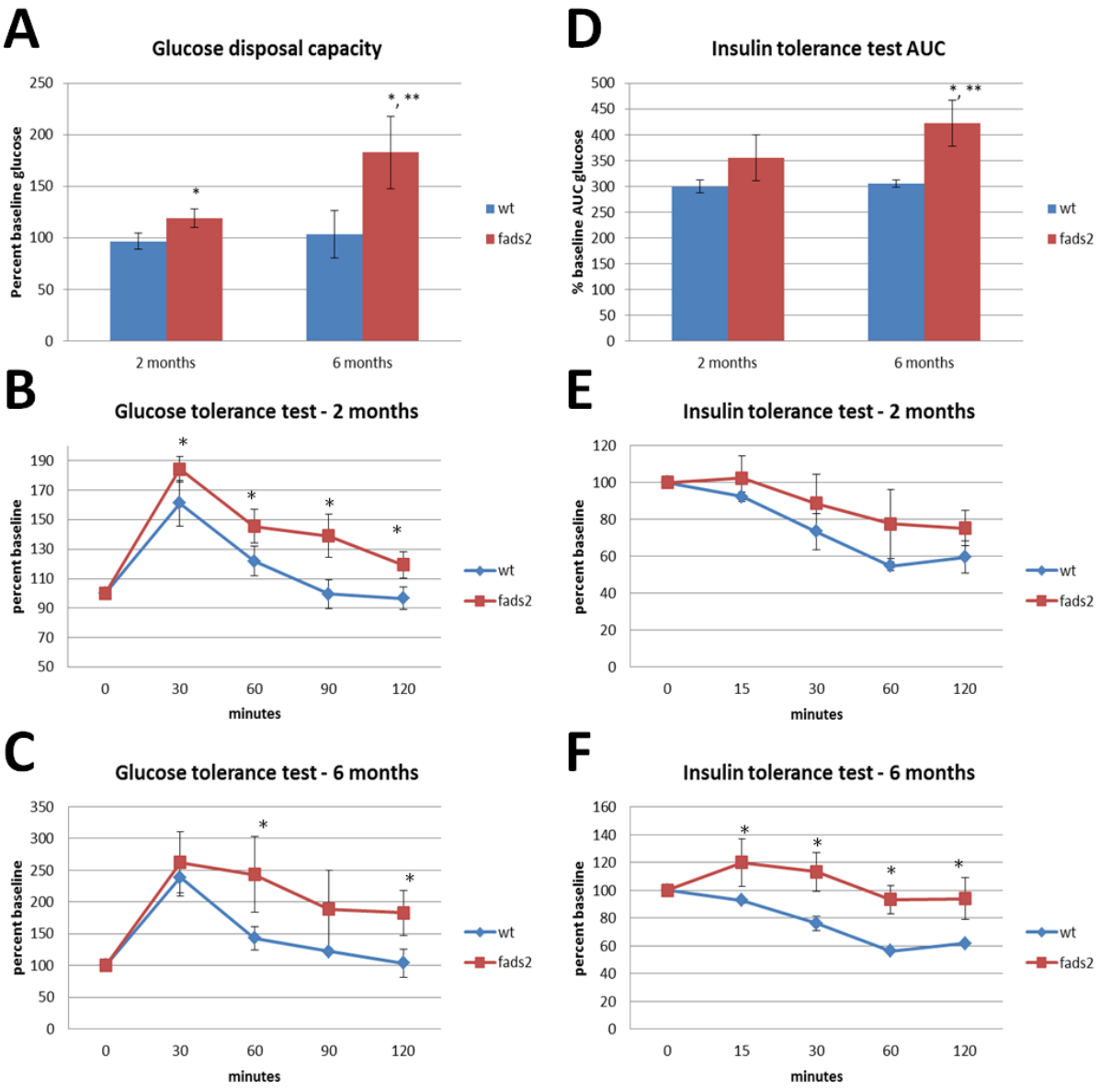

Figure 3.2 Glucose and insulin tolerance in mice genetically over-expressing *fads2 vs. wt.*

Genetic over-expression of *fads*2 impairs glucose tolerance and insulin sensitivity. (A) Glucose disposal capacity. (B) Glucose tolerance test (GTT) at 2 months of age. (C) GTT at 6 months of age. (D) Insulin tolerance test (ITT) area under the curve (AUC). (E) ITT at 2 months of age. (F) ITT at 6 months of age. One (*) denotes significant difference from wt, $p<0.05$ and two (**) denotes significant difference with age, $p<0.05$.

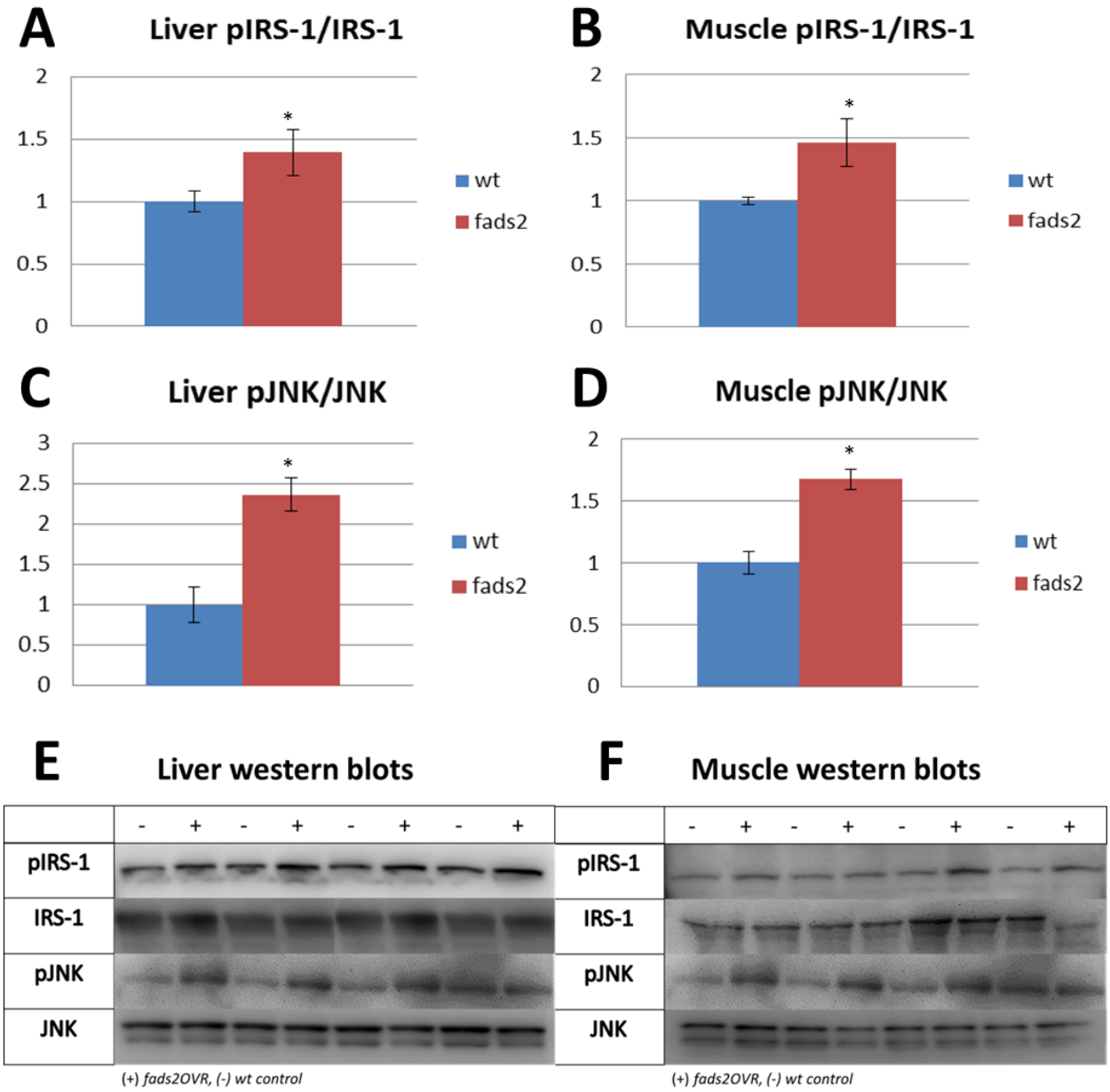

Figure 3.3 *fads2* over-expression results in increased pJNK and pIRS-1 content in liver and muscle. Genetic over-expression of *fads2* significantly increased pJNK, and pIRS-1 protein content in liver and muscle compared to wt controls. There was no significant difference between groups for JNK and IRS-1. Data are presented as phospho protein/ non-phospho protein. (*) denotes significance $p<0.05$.

Discussion

This study provides significant evidence for the ability of over-expression of D6D, the rate limiting enzyme in the synthesis of highly unsaturated fatty acids, independent of any other pathology, to augment systemic inflammation and initiate the development of metabolic insults associated with T2D. Although previous studies have linked D6D activity with markers and incidence of insulin resistance and T2D this is the first study to show experimentally that increasing D6D activity can independently result in these metabolic abnormalities.

As hypothesized global over-expression of *fads2*, the gene that encodes for D6D, led to significant increases in the AA/LA ratio in serum, heart, liver, and muscle and significant increases in AA derived pro-inflammatory eicosanoids. Our data suggests that one of the mechanisms by which D6D leads to impaired glucose homeostasis is through inflammation initiated insulin signaling impairment. It has been well established that serine phosphorylation of insulin receptor substrate 1 (IRS-1) by activated JNK impairs the insulin signaling cascade and that JNK is activated by pro-inflammatory cytokines and free fatty acid, such as AA(31, 39). In our model of *fads2OVR* serine phosphorylated IRS-1 and activated JNK were found to be significantly elevated in the liver and muscle. Elevations in these proteins were associated with significant developments of glucose and insulin intolerance. Glucose and insulin tolerance began to decline at an early age and progressed to a severe intolerance as the animals aged.

Interestingly, *fads2OVR* also resulted in increased serum triglycerides, LDL/VLDL, and total cholesterol. A necessary step in the normal assembly and secretion of VLDL from the liver is the production of phosphatidylcholine (PC), the primary phospholipid in VLDL, by the enzyme phosphatidylethanolamine (PE) N-methyltransferase (PEMT)(40). PEMT catalyzes the conversion of PE to PC for hepatic VLDL-TG assembly and secretion, and is known to require

substrate (PE) containing AA or DHA for conversion to (PC)(41, 42). This indicates that long-chain PUFAs, derived either from the diet or by de novo production by the D6D pathway, are necessary for normal lipid secretion. Therefore, D6D hyperactivity increases production of substrate for PEMT, which could lead to increased VLDL-triglyceride secretion. Taken together, this strongly suggests a link between the metabolism of essential n3 and n6 PUFAs to their LC-PUFA derivative and the increased production and secretion of VLDL-TG seen in metabolic syndrome. Future studies have been proposed in grants currently being reviewed to investigate the role of D6D as an important regulator of hepatic VLDL synthesis and secretion.

CHAPTER IV – OVERALL CONCLUSIONS

This collection of work provides extensive experimental evidence supporting the contribution of D6D activity to the development of insults associated with heart failure and T2D. With the use of the orally active pharmacological D6D inhibitor SC-26196 we found that D6D is an important modulator of cardiac hypertrophy and function in animal models of heart failure. We also found that by inhibiting D6D in the ob/ob mouse, a model of insulin resistance/Type 2 Diabetes, glucose tolerance was improved and the production of pro-inflammatory eicosanoids derivatives was reduced. Furthermore, the reduction in circulating eicosanoids was associated with a reduction in pJNK and pIRS-1, proteins shown to be involved in impaired insulin signaling. Given these findings occurred in the presence of associated pathology it could be concluded that D6D contributed to the development of the disease. To determine whether elevated D6D activity was a driver of the pathology we began to phenotype the *fads2OVR* mouse. Initial phenotyping efforts were focused on diabetes related outcomes. We found that over-expression of D6D in the absence of any overt pathology can lead to the development of significant glucose and insulin intolerance. There was also a significant increase in circulating lipids and pro-inflammatory eicosanoids which we believe played a role in the activation of the JNK signaling cascade leading to impaired insulin signaling.

Based on the findings of these studies it is apparent that, whether pathological or genetic, an elevation in D6D activity can increase the risk of the development of complications associated with cardiovascular disease and T2D. While these studies shed light on the mechanisms behind D6D role in disease more research is needed to determine which pathways mediate development and the progression of the pathology. These findings hopefully will provide another factor that

can be taken into consideration when treating diseases that have been associated with elevated D6D activity.

Future Directions

To further understand the biological significance of delta-6-desaturase in health and disease we will continue to characterize the *fads2OVR* mouse model as it relates to insults associated with Type 2 Diabetes and Cardiovascular disease. Also, in light of our interesting finding that over-expression of D6D leads to elevated blood lipid levels, most notably triglycerides and VLDL possible mechanisms behind this result and other disease states associated with elevated blood lipids, such as atherosclerosis will be explored. Finally, work will continue with a drug discovery group to try to develop a more potent pharmacological D6D inhibitor that may eventually be used in human treatment of disease.

REFERENCES

1. Warensjo E, *et al.* (2009) Associations between estimated fatty acid desaturase activities in serum lipids and adipose tissue in humans: links to obesity and insulin resistance. *Lipids in health and disease* 8:37.
2. Park H, *et al.* (The fatty acid composition of plasma cholesteryl esters and estimated desaturase activities in patients with nonalcoholic fatty liver disease and the effect of long-term ezetimibe therapy on these levels. *Clin Chim Acta* 411(21-22):1735-1740.
3. Decsi T, Molnar D, & Koletzko B (1996) Long-chain polyunsaturated fatty acids in plasma lipids of obese children. *Lipids* 31(3):305-311.
4. Decsi T, Molnar D, & Koletzko B (1998) The effect of under- and overnutrition on essential fatty acid metabolism in childhood. *European journal of clinical nutrition* 52(8):541-548.
5. Laaksonen DE, *et al.* (2002) Serum fatty acid composition predicts development of impaired fasting glycaemia and diabetes in middle-aged men. *Diabetic medicine : a journal of the British Diabetic Association* 19(6):456-464.
6. Hodge AM, *et al.* (2007) Plasma phospholipid and dietary fatty acids as predictors of type 2 diabetes: interpreting the role of linoleic acid. *The American journal of clinical nutrition* 86(1):189-197.
7. Kroger J, *et al.* (Erythrocyte membrane phospholipid fatty acids, desaturase activity, and dietary fatty acids in relation to risk of type 2 diabetes in the European Prospective Investigation into Cancer and Nutrition (EPIC)-Potsdam Study. *Am J Clin Nutr* 93(1):127-142.
8. Decsi T, *et al.* (2000) Polyunsaturated fatty acids in plasma lipids of obese children with and without metabolic cardiovascular syndrome. *Lipids* 35(11):1179-1184.
9. Kawashima A, *et al.* (2009) Plasma fatty acid composition, estimated desaturase activities, and intakes of energy and nutrient in Japanese men with abdominal obesity or metabolic syndrome. *Journal of nutritional science and vitaminology* 55(5):400-406.
10. Vessby B (2003) Dietary fat, fatty acid composition in plasma and the metabolic syndrome. *Current opinion in lipidology* 14(1):15-19.
11. Warensjo E, Riserus U, & Vessby B (2005) Fatty acid composition of serum lipids predicts the development of the metabolic syndrome in men. *Diabetologia* 48(10):1999-2005.
12. Colas R, *et al.* (Increased lipid peroxidation in LDL from type-2 diabetic patients. *Lipids* 45(8):723-731.
13. Martinelli N, *et al.* (2008) FADS genotypes and desaturase activity estimated by the ratio of arachidonic acid to linoleic acid are associated with inflammation and coronary artery disease. *The American journal of clinical nutrition* 88(4):941-949.
14. Warensjo E, Sundstrom J, Vessby B, Cederholm T, & Riserus U (2008) Markers of dietary fat quality and fatty acid desaturation as predictors of total and cardiovascular mortality: a population-based prospective study. *The American journal of clinical nutrition* 88(1):203-209.
15. Erkkila A, de Mello VD, Riserus U, & Laaksonen DE (2008) Dietary fatty acids and cardiovascular disease: an epidemiological approach. *Progress in lipid research* 47(3):172-187.

16. Malerba G, *et al.* (2008) SNPs of the FADS gene cluster are associated with polyunsaturated fatty acids in a cohort of patients with cardiovascular disease. *Lipids* 43(4):289-299.
17. Nakamura MT & Nara TY (2004) Structure, function, and dietary regulation of delta6, delta5, and delta9 desaturases. *Annual review of nutrition* 24:345-376.
18. Heyen JR, *et al.* (2002) Structural, functional, and molecular characterization of the SHHF model of heart failure. *American journal of physiology. Heart and circulatory physiology* 283(5):H1775-1784.
19. Sparagna GC, *et al.* (2007) Loss of cardiac tetralinoleoyl cardiolipin in human and experimental heart failure. *Journal of lipid research* 48(7):1559-1570.
20. Obukowicz MG, *et al.* (1998) Novel, selective delta6 or delta5 fatty acid desaturase inhibitors as antiinflammatory agents in mice. *The Journal of pharmacology and experimental therapeutics* 287(1):157-166.
21. Mulligan CM, *et al.* (2012) Dietary linoleate preserves cardiolipin and attenuates mitochondrial dysfunction in the failing rat heart. *Cardiovascular research* 94(3):460-468.
22. Zarini S, Gijon MA, Ransome AE, Murphy RC, & Sala A (2009) Transcellular biosynthesis of cysteinyl leukotrienes in vivo during mouse peritoneal inflammation. *Proceedings of the National Academy of Sciences of the United States of America* 106(20):8296-8301.
23. Leslie CC (2004) Regulation of arachidonic acid availability for eicosanoid production. *Biochemistry and cell biology = Biochimie et biologie cellulaire* 82(1):1-17.
24. Jenkins CM, Cedars A, & Gross RW (2009) Eicosanoid signalling pathways in the heart. *Cardiovascular research* 82(2):240-249.
25. Le CH, *et al.* (2014) Delta-6-desaturase links polyunsaturated fatty acid metabolism with phospholipid remodeling and disease progression in heart failure. *Circulation. Heart failure* 7(1):172-183.
26. Murphy RC, *et al.* (2005) Electrospray ionization and tandem mass spectrometry of eicosanoids. *Analytical biochemistry* 346(1):1-42.
27. Kurotani K, *et al.* (2012) High levels of stearic acid, palmitoleic acid, and dihomo-gamma-linolenic acid and low levels of linoleic acid in serum cholesterol ester are associated with high insulin resistance. *Nutr Res* 32(9):669-675 e663.
28. Shindou H & Shimizu T (2009) Acyl-CoA:lysophospholipid acyltransferases. *The Journal of biological chemistry* 284(1):1-5.
29. Kayama Y, *et al.* (2009) Cardiac 12/15 lipoxygenase-induced inflammation is involved in heart failure. *The Journal of experimental medicine* 206(7):1565-1574.
30. Zhang Z, *et al.* (2003) COX-2-dependent cardiac failure in Gh/tTG transgenic mice. *Circulation research* 92(10):1153-1161.
31. Tarantino G & Caputi A (2011) JNKs, insulin resistance and inflammation: A possible link between NAFLD and coronary artery disease. *World journal of gastroenterology : WJG* 17(33):3785-3794.
32. Brenner RR, *et al.* (2003) Desaturase activities in rat model of insulin resistance induced by a sucrose-rich diet. *Lipids* 38(7):733-742.
33. Montanaro MA, *et al.* (2005) Effect of troglitazone on the desaturases in a rat model of insulin-resistance induced by a sucrose-rich diet. *Prostaglandins, leukotrienes, and essential fatty acids* 72(4):241-250.

34. Osada K, Kodama T, Yamada K, Nakamura S, & Sugano M (1998) Dietary oxidized cholesterol modulates cholesterol metabolism and linoleic acid desaturation in rats fed high-cholesterol diets. *Lipids* 33(8):757-764.
35. Garg ML, Thomson AB, & Clandinin MT (1990) Interactions of saturated, n-6 and n-3 polyunsaturated fatty acids to modulate arachidonic acid metabolism. *Journal of lipid research* 31(2):271-277.
36. Brenner RR (1981) Nutritional and hormonal factors influencing desaturation of essential fatty acids. *Progress in lipid research* 20:41-47.
37. Brenner RR (2003) Hormonal modulation of delta6 and delta5 desaturases: case of diabetes. *Prostaglandins, leukotrienes, and essential fatty acids* 68(2):151-162.
38. Eck MG, Wynn JO, Carter WJ, & Faas FH (1979) Fatty acid desaturation in experimental diabetes mellitus. *Diabetes* 28(5):479-485.
39. Rizzo MT & Carlo-Stella C (1996) Arachidonic acid mediates interleukin-1 and tumor necrosis factor-alpha-induced activation of the c-jun amino-terminal kinases in stromal cells. *Blood* 88(10):3792-3800.
40. Noga AA, Zhao Y, & Vance DE (2002) An unexpected requirement for phosphatidylethanolamine N-methyltransferase in the secretion of very low density lipoproteins. *The Journal of biological chemistry* 277(44):42358-42365.
41. DeLong CJ, Shen YJ, Thomas MJ, & Cui Z (1999) Molecular distinction of phosphatidylcholine synthesis between the CDP-choline pathway and phosphatidylethanolamine methylation pathway. *The Journal of biological chemistry* 274(42):29683-29688.
42. Watkins SM, Zhu X, & Zeisel SH (2003) Phosphatidylethanolamine-N-methyltransferase activity and dietary choline regulate liver-plasma lipid flux and essential fatty acid metabolism in mice. *The Journal of nutrition* 133(11):3386-3391.

APPENDIX I

Lipid analysis method

To determine the global fatty acid profile of tissue phospholipids 600 µl of methanol (precooled to 4°C) was added to 20-50 µl of serum sample in an eppendorf tube. For tissue samples ~20mg of liver, ~10mg of heart, ~20mg of muscle was homogenized in 800µl of methanol in glass homogenizer then the homogenate was transferred to an eppendorf tube. Samples were vortexed for ~30 seconds and centrifuged at 900g(~3200rpm) for 5 min. 25 µl of sodium methoxide solution was added to a (13X100mm) glass tube for each sample. The methanol supernatant from the centrifuge tube was added to the corresponding glass tube for that sample. Samples were vortexed ~30 seconds to allow the selective synthesis of methyl esters from glycerophospholipids fatty acids. The reaction was left to occur for 3 minutes at room temperature. The reaction was stopped after 3 minutes by adding 75 µl of methanolic HCl to each glass tube. The fatty acid methyl esters (FAMEs) were extracted by adding 700 µl of Hexane to each tube and vortexed for ~30 seconds. Using a glass pipet the upper hexane layer (containing the FAMEs) was transferred into a 2 ml GC vial. The extraction was repeated with another 700 µl of hexane, and combined with the previous extract. Samples were then dried under nitrogen flow and re-suspended in hexane for gas chromatography analysis.

GC analysis was performed using an Agilent Technologies DB-225 30m x 0.250mm x 0.25µm column (model 122-2232, J&W Scientific) on an Agilent 6890 Series Gas Chromatographer. The initial temperature of the oven was 120 °C with an initial ramp temperature of 10°C/min for 8 minutes, then 2.5°C/min for 4 minutes and held at 210°C for the remaining 6 minutes for a total run time of 20 min. The inlet split ratio was 15:1 with the column

at constant flow and an initial flow, pressure, and velocity at1.8ml/min, 23.59 psi, and 42 cm/sec, respectively.

Phospholipid class separation

Phospholipids (PE, PC, PI and CL) were separated by normal phase HPLC (Agilent Rx-sil colum; 4.6X250mm) using two mobile phases: Solvent A, Hexane:IPA:0.3mM Potassium Acetate (pH 7.0):acetic acid (42.4:56.6:1:0.01) and Solvent B, Hexane:IPA:5mM Potassium Acetate (pH 7.0):Acetic Acid (38.6:51.4:10:0.1), the percentages of each were varied throughout the 18 min run (flow rate 1.5ml/min) to resolve (206nm) and collect individual phospholipid (PL) fractions.

Immunoblotting method

Tissue Preparations

Frozen tissue sections were chipped, weighed, and then immediately immersed in homogenization buffer at 1:10 w/v. Homogenization buffer consisted of MPER lysis buffer containing a phosphatase inhibitor cocktail. Tissues were homogenized in buffer using glass on glass tissue grinder mortar and pestle on ice. Following homogenization, samples were centrifuged for 10minutes at 4C. After centrifugation, supernatants were transferred to new eppendorf tubes and pellets were stored at -80C. Supernatant samples containing proteins of interest were then sonicated and protein concentrations were measured by BCA assay (Thermo Sci, Catalog #23225). Following protein quantification, samples were either immediately used for immunoblotting or stored at -80C until further use.

Buffer Preparations

All buffers we prepared and diluted according to manufacturer's directions. Both stock solutions of running buffer and transfer buffer were prepared as 10X solutions and stored at room temperature prior to use. Stock solution of Running Buffer consisted of 10X Tris/Glycine/SDS Buffer (BioRad, Catalog #161-0732). Stock solution of Transfer Buffer was made with 24.7 mM Tris and 191.8 mM
Glycine diluted in water to a 10X concentration. Working Running Buffer was prepared to a 1X concentration. Working Transfer Buffer was prepared at a 1500mL volume composed of 300mL methanol, 150mL 10X Transfer Buffer, and 1050uL milliQ water. Prior to use, working transfer buffer was chilled for approximately 45 minutes at 4C. Wash buffer was composed of 1X TBS with 0.1% Tween-20.

Primary and Secondary Antibody Preparations

Antibodies designed to probe for proteins of interest were purchased from one of several manufacturers (AbCam, Abnova, Calbiochem, Cell Signaling ThermoScientific) and stored according to manufacturer's instructions at 4C, - 20C, or -80C. Dilutions were performed per included instructions and optimized to appropriate concentrations for detection in mouse tissue (Table 1). Primary antibodies were diluted in either 5% nonfat milk or BSA dependent on manufacturer specifications. Species-specific secondary antibodies were used at previously determined dilutions and were diluted in either 1% nonfat milk or BSA dependent on manufacturer instructions.

Electrophoresis Gels

2X Laemlli SDS Loading Buffer was added to diluted tissue samples containing 50ug of protein. Protein concentrations of each sample were determined by the BCA protein plate assay. Precast 4-20% Tris-HCl 26-lane gels were purchased from BioRad (Catalog#345-0034) and 15uL of sample with Laemelli loading buffer was added to each well. Additionally, 5uL of Western Protein Standard (BioRad, Catalog #161-0376) was loaded in predetermined lanes for use as a molecular weight marker.

Incubation Times and Temperatures

Gels were run in Running Buffer for approximately 45 minutes at 200V. Following gel electrophoresis, proteins were transferred onto PVDF membranes (Millipore, Catalog #ISEQ00010) in Transfer Buffer for 1hour at 100V. PVDF membranes were washed several times with milliQ water and then blocked at room temperature for 1 hour in either 5% non-fat milk or BSA according to primary antibody manufacturer's instructions. Membranes were incubated in properly diluted primary antibody overnight at 4C. Following overnight incubation, membranes were washed 6 times for 5 minutes with Wash Buffer. Membranes were incubated in diluted secondary antibody for 1-hour at room temperature. Membranes were washed as before and coated with chemiluminescent substrates for 5 minutes. AP-conjugated secondary antibodies were incubated in Immuno-Star AP Substrate (BioRad, Catalog #170-5018. Membranes were visualized using a UVP developer and exposed for several minutes until bands fluoresced at optimal levels.

Quantification of Bands

Immunoblotting results were quantified using the NIH provided software, ImageJ. Results are expressed in relative units (RU) as fold changes versus control (con) mouse levels.

Table A1. Total phospholipid fatty acid composition for serum, liver, muscle and heart

	Serum-WT	**Serum-*fads2***		**Liver-WT**	**Liver-*fads2***	
	(%)	**(%)**	**(P)**	**(%)**	**(%)**	**(*P*)**
16:0, Palmitic	21.73 ± 0.01	21.23 ± 0.58	0.207	21.24 ± 0.33	20.53 ± 0.06	0.035
16:1, Palmitoleic	1.15 ± 0.07	1.94 ± 0.23	0.017	1.39 ± 0.31	1.43 ± 0.08	0.449
18:0, Stearic	8.44 ± 0.53	8.86 ± 0.45	0.254	13.77 ± 0.52	14.19 ± 0.36	0.224
18:1n9, Oleic	19.14 ± 0.22	20.75 ± 0.96	0.085	14.37 ± 1.35	13.31 ± 0.60	0.218
18:1n7, Vaccenic	1.92 ± 0.18	2.90 ± 0.22	0.014	1.90 ± 0.09	2.30 ± 0.09	0.006
18:2n6, Linoleic	35.49 ± 1.35	30.77 ± 0.79	0.016	23.70 ± 0.15	22.38 ± 0.58	0.012
18:3n3, Linolenic	1.99 ± 0.14	1.36 ± 0.12	0.012	0.64 ± 0.00	0.55 ± 0.00	0.000
20:3n6, DHGLA	0.68 ± 0.04	0.98 ± 0.01	0.001	1.05 ± 0.05	1.24 ± 0.15	0.074
20:4n6, AA	6.49 ± 0.60	7.32 ± 0.30	0.108	13.46 ± 0.93	14.94 ± 0.33	0.075
20:5n3, EPA	0.17 ± 0.01	0.23 ± 0.03	0.062	0.16 ± 0.02	0.21 ± 0.02	0.033
22:5n3, DPA	0.28 ± 0.02	0.27 ± 0.03	0.382	0.35 ± 0.02	0.32 ± 0.02	0.055
22:6n3, DHA	2.52 ± 0.29	3.39 ± 0.33	0.051	7.96 ± 0.69	8.61 ± 0.20	0.173
AA/LA	0.18 ± 0.02	0.24 ± 0.01	0.036	0.57 ± 0.04	0.67 ± 0.03	0.038
DHA/ALA	1.28 ± 0.24	2.49 ± 0.18	0.008	12.44 ± 1.15	15.66 ± 0.43	0.018

	Muscle-WT	**Muscle-*fads2***		**Heart-WT**	**Heart-*fads2***	
	(%)	**(%)**	**(P)**	**(%)**	**(%)**	**(*P*)**
16:0, Palmitic	22.02 ± 0.03	22.77 ± 0.41	0.103	15.40 ± 0.01	14.20 ± 0.30	0.028
16:1, Palmitoleic	3.81 ± 0.27	5.79 ± 0.83	0.075	0.78 ± 0.01	0.47 ± 0.12	0.061
18:0, Stearic	6.85 ± 0.45	7.79 ± 0.02	0.088	18.25 ± 0.05	18.60 ± 0.04	0.014
18:1n9, Oleic	19.24 ± 1.15	15.11 ± 0.22	0.036	9.08 ± 0.05	7.92 ± 0.09	0.004
18:1n7, Vaccenic	2.58 ± 0.09	2.64 ± 0.01	0.311	1.94 ± 0.11	1.95 ± 0.05	0.464
18:2n6, Linoleic	26.04 ± 0.50	21.66 ± 0.96	0.028	21.44 ± 0.10	20.13 ± 0.48	0.057
18:3n3, Linolenic	1.19 ± 0.07	1.23 ± 0.01	0.300	0.39 ± 0.01	0.34 ± 0.00	0.016
20:3n6, DHGLA	0.50 ± 0.01	0.52 ± 0.01	0.171	0.59 ± 0.01	0.74 ± 0.02	0.009
20:4n6, AA	7.51 ± 0.34	8.31 ± 0.13	0.078	8.06 ± 0.12	8.83 ± 0.37	0.093
20:5n3, EPA	0.08 ± 0.00	0.10 ± 0.01	0.046	0.03 ± 0.00	0.04 ± 0.00	0.116
22:5n3, DPA	1.02 ± 0.11	1.22 ± 0.01	0.115	1.30 ± 0.02	1.20 ± 0.02	0.040
22:6n3, DHA	9.14 ± 1.17	12.85 ± 0.13	0.044	22.75 ± 0.12	25.60 ± 0.60	0.022
AA/LA	0.29 ± 0.01	0.38 ± 0.02	0.028	0.38 ± 0.01	0.44 ± 0.01	0.014
DHA/ALA	7.63 ± 0.55	10.42 ± 0.05	0.019	58.98 ± 1.66	76.28 ± 1.09	0.006